AGU PUBLICATIONS

Geophysical Research Letters

RESEARCH LETTER
10.1002/2015GL065066

Key Points:
- Meteor radar echo decay times can be used to estimate the height of a constant density level
- The meteor radar decay time gradient reverses around 1.26E−5 kg/m3
- Airglow layer height can be estimated using meteor radar data

Correspondence to:
J. P. Younger,
joel.younger@adelaide.edu.au

Citation:
Younger, J. P., I. M. Reid, R. A. Vincent, and D. J. Murphy (2015), A method for estimating the height of a mesospheric density level using meteor radar, *Geophys. Res. Lett.*, *42*, 6106–6111, doi:10.1002/2015GL065066.

Received 23 JUN 2015
Accepted 4 JUL 2015
Accepted article online 7 JUL 2015
Published online 24 JUL 2015

A method for estimating the height of a mesospheric density level using meteor radar

J. P. Younger[1,2], I. M. Reid[1,2], R. A. Vincent[2], and D. J. Murphy[3]

[1] ATRAD Pty Ltd., Thebarton, South Australia, Australia, [2]School of Physical Sciences, University of Adelaide, Adelaide, South Australia, Australia, [3]Australian Antarctic Division, Kingston, Tasmania, Australia

Abstract A new technique for determining the height of a constant density surface at altitudes of 78–85 km is presented. The first results are derived from a decade of observations by a meteor radar located at Davis Station in Antarctica and are compared with observations from the Microwave Limb Sounder instrument aboard the Aura satellite. The density of the neutral atmosphere in the mesosphere/lower thermosphere region around 70–110 km is an essential parameter for interpreting airglow-derived atmospheric temperatures, planning atmospheric entry maneuvers of returning spacecraft, and understanding the response of climate to different stimuli. This region is not well characterized, however, due to inaccessibility combined with a lack of consistent strong atmospheric radar scattering mechanisms. Recent advances in the analysis of detection records from high-performance meteor radars provide new opportunities to obtain atmospheric density estimates at high time resolutions in the MLT region using the durations and heights of faint radar echoes from meteor trails. Previous studies have indicated that the expected increase in underdense meteor radar echo decay times with decreasing altitude is reversed in the lower part of the meteor ablation region due to the neutralization of meteor plasma. The height at which the gradient of meteor echo decay times reverses is found to occur at a fixed atmospheric density. Thus, the gradient reversal height of meteor radar diffusion coefficient profiles can be used to infer the height of a constant density level, enabling the observation of mesospheric density variations using meteor radar.

1. Introduction

The density of the neutral atmosphere in the mesosphere/lower thermosphere (MLT) region around 80–100 km is difficult to measure, due to the lack of strong radar scattering mechanisms and the high altitude. Lidar can provide measurements up to the lower part of the MLT region, but expense, complexity, and difficulty making measurements in daylight and poor weather prohibit their use for routine monitoring. Satellite instruments, while often having near-global coverage, sample individual locations infrequently. Sounding rockets can produce density profiles by tracking the descent speed of ejected spheres [*Lübken et al.*, 2004], but the requirements of launching high-altitude rockets limits their use to focused campaigns. There remains a need for a density measurement technique capable of operating continuously in all conditions at fixed locations.

The immediate benefit of density observations will be their use as a tool for studying the climate and dynamics of the middle atmosphere, including both long-term changes and short-term wave-driven variability. Density measurements in the MLT provide particular benefit to the interpretation of airglow measurements of atmospheric temperature, which use chemiluminescent emissions from species including O, O_2, and OH [*Takahashi et al.*, 2004]. Furthermore, density governs the deceleration and ablation of objects entering the atmosphere. Dynamical studies of meteoric ablation and the terminal entry behavior of space debris require knowledge of density in the MLT, providing applications in the space situational awareness field. Spacecraft entry planning requires accurate knowledge of atmospheric density to achieve a desired landing area, particularly for vehicles with aerodynamic control surfaces that become usable within the MLT region.

The decay times of radar echoes from underdense meteor trails have been used for decades as a tool to infer the temperature of the atmosphere in the MLT. Recent advances in meteor radar performance have enabled the detection of meteors well below the peak detection height of about 90 km. Analysis of meteors in the lowest portion of the meteor ablation region, below about 85 km, indicates that there is significant deviation in meteor plasma behavior from theoretical predictions based only on ambipolar diffusion [*Kim et al.*, 2010].

Younger et al. [2014] showed that the unexpected reduction in meteor radar echo decay times in the lower portion of the meteor ablation region is due to the neutralization of meteoric plasma through a number of chemical reactions with the background atmosphere. This effect is sufficient to reverse the usual behavior of meteor radar echo decay times, with echoes below some critical height having smaller durations with decreasing altitude. *Younger et al.* [2014] found that the height at which the echo decay time gradient reverses appears to be correlated to a constant value of atmospheric density.

Thus, while plasma neutralization makes low-altitude meteor echoes unsuitable for atmospheric temperature measurements, the height at which the decay time gradient reverses can be used to determine the height of a constant density surface. Here we examine this relationship in detail to assess the feasibility of using low-altitude meteor radar decay times as a tool for inferring atmospheric density. The source data include a decade of Antarctic meteor radar observations and measurements from the Microwave Limb Sounder aboard the Earth Observing System Aura satellite.

2. Meteor Radar

When objects enter the atmosphere from heliocentric orbits at relative velocities of 11–70+ km s^{-1}, the resultant heating results in a narrow column of ionized evaporated material behind the meteoroid at heights between 70 and 110 km. Meteor radars use the plasma of meteor trails for scattering targets in the MLT region. As meteor plasma drifts with background winds, the change in phase of radiowave backscatter from meteor trails can be used to deduce wind speed and direction. *Jones et al.* [1998] describe the most common configuration for meteor radar, including a single all-sky transmitting antenna and an interferometer composed of two perpendicular baselines, each with two antenna pairs spaced at 2.0 and 2.5 times the radar wavelength. The angle of arrival of incident radio waves scattered by a meteor trail is determined from the comparison of the differences in the phase of the echo between different antenna pairs [*Holdsworth*, 2005].

Meteor radar detections were obtained for the decade 2005–2014 using a 33 MHz ATRAD Meteor Detection Radar operated by the Australian Antarctic Division at Davis Station, Antarctica (68.5°S, 77.9°E). Installed in 2004, the 33 MHz meteor radar transmits 3.6 km long, 4 bits complimentary coded circularly polarized pulses at a pulse repetition rate of 430 Hz [*Holdsworth et al.*, 2008]. The radar is configured primarily for the determination of winds in the MLT region using the phase drift of echoes from underdense meteor trails.

The typical meteor detection rate of the Davis Station 33 MHz meteor radar is 5000–15,000 unambiguous underdense meteor detections per day, with variability primarily driven by diurnal and seasonal changes to the orientation of the Antarctic observing location with respect to the dominant meteor sources in space [*Campbell-Brown*, 2008]. The height of a meteor radar detection at range R and angle θ from the zenith is determined using the relation $h = \sqrt{R_E^2 + R^2 + 2RR_E \cos\theta} - R_E$, where R_E is the radius of Earth. As uncertainty in range measurements is fixed, the uncertainty in height for detections closer to the horizon is dominated by zenith angle uncertainty. In order to avoid the possibility of excessive error in the height estimates of individual meteors, detections for this study were restricted to meteors detected at zenith angles of less than 60°, which reduced the effective daily detection rate to 4000–10,000 $days^{-1}$.

3. Diffusion Coefficient Estimates From Meteor Radar

Underdense meteor trails, which have linear plasma densities along the trail axis of less than about 2.4×10^{14} el m^{-1} [*McKinley*, 1961], scatter radiowaves throughout their volume. Coherent addition of radiowaves scattered from individual electrons produces highly specular echoes, with the passage of an ablating meteoroid across the field of view of a radar resulting in the observed backscatter intensity over time producing a knife-edge diffraction pattern.

As the plasma of the trail diffuses outward from the trail axis into the surrounding atmosphere, an increase in destructive interference and reduction in backscatter from the core of the trail causes radar echo power to decrease exponentially with time. Thus, the time, τ, taken for the intensity of a radar echo from an underdense meteor trail to decay to a factor of e^{-1} of the original maximum received power can be used to infer the ambipolar diffusion coefficient, D, of the atmosphere from the relation

$$D = \frac{\lambda^2}{16\pi^2\tau}, \tag{1}$$

where λ is the transmitting wavelength of the observing radar [*Herlofson*, 1947]. Diffusion coefficient estimates are used in place of meteor echo decay times throughout this study to facilitate direct comparison with alternative sensors.

The ambipolar diffusion coefficient is a valuable metric, as it is a function of atmospheric temperature, T, atmospheric pressure, p, or density, ρ, and the mobility, K_0, of the ions in the meteoric plasma, as given by

$$D = 6.39 \times 10^{-2} K_0 \frac{T^2}{p} = 2.23 \times 10^{-4} K_0 \frac{T}{\rho}. \quad (2)$$

From a physical perspective, D describes the rate at which a plasma in thermal equilibrium diffuses into the background medium of the neutral atmosphere based on a collisional random walk. Separation of charge is inhibited by the rise of electric fields between ions and free electrons, so the rate of the diffusive process is driven by the collision frequency of plasma ions and atmospheric molecules. Useful in its own right as a diagnostic of plasma behavior in the MLT, D can theoretically also be combined with supplied values of p to recover atmospheric temperature [*Tsutsumi et al.*, 1994]. Alternatively, the gradient $\mathrm{d}/\mathrm{d}z \log D$ can be used with supplied values of the temperature gradient $\mathrm{d}T/\mathrm{d}z$ to determine T [*Hocking*, 1999].

For radar-only analyses, meteor detections were binned into 4 h blocks to avoid excessive variation due to semidiurnal and diurnal tides. Within each 4 h segment, the mean diffusion coefficient was calculated in 1 km bins to produce profiles of D with respect to z. A rudimentary outlier rejection was applied, in which diffusion coefficients more than two standard deviations from the mean were discarded and a new mean calculated from the remaining estimates in each height bin.

4. Aura Satellite MLS Data

Neutral atmospheric density and independent estimates of D were obtained from Aura satellite observations of the atmospheric column near Davis Station, Antarctica. The Aura satellite, launched in 2004, is a part of the A-Train constellation of Earth-observing satellites, which also includes GCOM-W1, Aqua, CALIPSO, CloudSat, and OCO-2. The near-polar Sun-synchronous orbit facilitates two observation periods near the same location for each day, one on the ascending latitude leg of the orbit and the other on the descending latitude leg. The suite of instruments aboard Aura includes the Microwave Limb Sounder, which measures atmospheric emissions in the 118 GHz to 2.5 THz range to infer the densities of a number of different atmospheric species, neutral temperature, and geopotential height. Each measurement profile consists of 55 points gridded to fixed pressure surfaces, which is repeated at a spacing of 165 km along the orbital track [*Waters et al.*, 2006].

Aura MLS data were restricted to observations made within a distance of 300 km of Davis Station, Antarctica, to keep satellite observations within the detection area of the meteor radar. For direct comparisons between meteor radar diffusion coefficient estimates and MLS observations, meteor detections were restricted to 6 h windows centered on Aura satellite overflight times. These constraints resulted in two sets of MLS observations near the meteor radar per 24 h period at approximately 10 h and 19 h local time.

Temperature and geopotential height measurements were used to construct MLS-based diffusion coefficient and density profiles. Geopotential heights were converted to geometric heights as described in *Younger et al.* [2014], with the radius of Earth at each observing latitude supplied by the WGS84 ellipsoid model [*Decker*, 1986]. The diffusion coefficient was calculated using equation (2) with an ionic mobility value of $K_0 = 2.5 \times 10^{-4}$ m^2 s^{-1} V^{-1} [*Chilson et al.*, 1996].

5. Low-Altitude Meteor Radar Diffusion Coefficients

The height at which $\mathrm{d}D/\mathrm{d}z = 0$ in the meteor radar profiles of D was determined by fitting a parabola to $\log D$ as a function of z in the region within ± 5 km of the minimum value of D. Uncertainty in the gradient reversal height, referred to as h_0 hereafter, was determined from the uncertainties of the fitted quadratic coefficients, assuming normal statistics for propagation of uncertainty.

Figure 1 shows the diffusion coefficient profile derived from Davis Station 33 MHz meteor radar data for a typical single 4 h period. The low-altitude curvature of the profile can clearly be seen, to which a fitted quadratic curve shows good agreement. A diffusion coefficient profile based on simultaneously gathered data from the MLS instrument aboard the Aura satellite is also shown, which demonstrates the dramatic

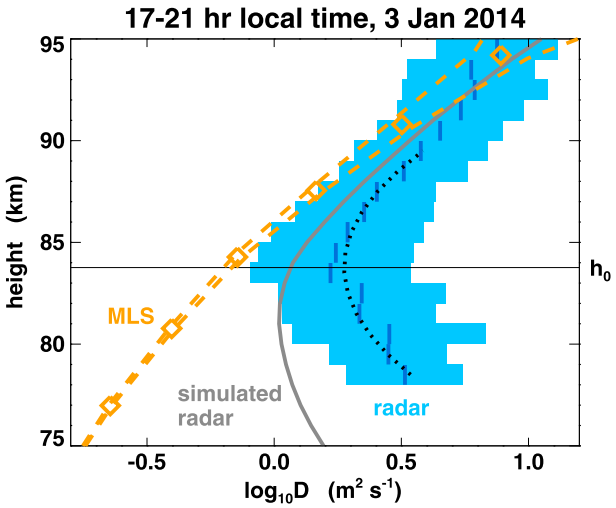

Figure 1. The diffusion coefficient profile for a single 4 h bin estimated from meteor radar echo decay times (blue line segments; bars show one standard deviation), Aura MLS observations (orange diamonds; dashed lines show one standard deviation), and a numerically simulated radar profile based on MLS data (solid gray line). The parabola fitted to meteor radar data used to determine h_0 is shown as a black dotted line.

departure from expected values of meteor radar-derived diffusion coefficients in the lower part of the meteor detection region.

A numerical simulation of the expected diffusion coefficient profile including plasma neutralization and chemical reactions [*Younger et al.*, 2014] shows reasonable qualitative agreement but fails to fully predict the reduction in echo decay times that produce the enhanced estimates of D made at low altitudes by the meteor radar. This is likely due to the conservative choices made for reaction rates and meteoric ions, in addition to the lack of hydrated ion chemistry in the model. As such, the simulated profile as presented should be seen as a theoretical floor for the effect of plasma neutralization and chemical reactions on meteor radar diffusion coefficient profiles.

The curve fitting algorithm was able to produce an estimate of the diffusion coefficient estimate gradient reversal height for more than 90% of the 4 h observation blocks. As shown in Figure 2, uncertainties in the estimate of h_0 were larger in winter months, which is not unexpected given that this time of year corresponds to the minimum meteor detection rate and an increase in atmospheric variability due to higher wave activity. The median uncertainty in estimates of h_0 was about 0.64 km, with 75% of the h_0 estimates having uncertainties less than 1 km.

For the period 2005–2014, a harmonic fit of h_0 yielded a mean value of 81.6 km with annual, semiannual, and terannual component amplitudes of 2.71 km, 0.55 km, and 0.16 km, respectively. The total range of the harmonic fit was 5.7 km, spanning 79.2–84.9 km. The mean absolute difference between the fitted value of h_0 and the harmonic fit was 0.80 km.

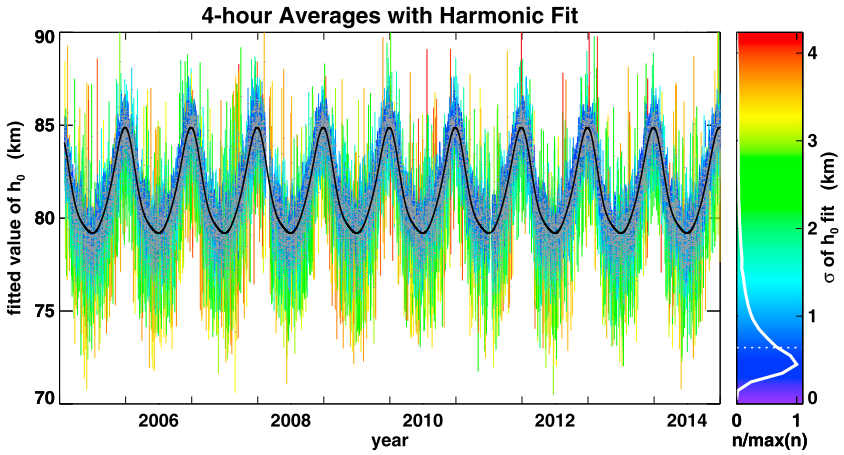

Figure 2. Heights at which the gradient of log D estimates reverse (gray points), as observed by the 33 MHz meteor radar at Davis Station, Antarctica. Fitted values of h_0 are taken from the average profiles in 4 h bins. Color-coded error bars show the one standard deviation range for each estimate of h_0. A harmonic fit of annual, semiannual, and terannual components is shown as a solid black line. The color legend also displays a histogram of the uncertainties in the fitted value of h_0 (solid white line), with the median value indicated by a dotted line.

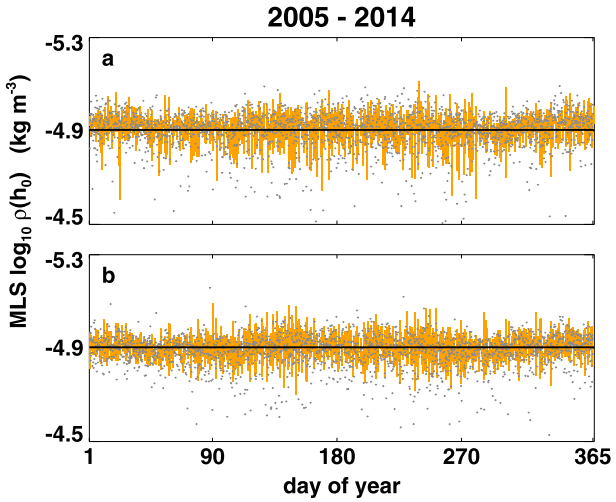

Figure 3. Neutral atmospheric density at h_0 derived from Aura MLS satellite observations. h_0 estimated in 6 h windows centered on Aura overflight times within 300 km of the Davis Station meteor radar. Gray points show individual density estimates, and orange error bars show the one standard deviation range for each day of the year averaged over 2005–2014. (a) Density obtained from the ascending latitude orbital leg. (b) Observations from the descending latitude orbital leg. The solid line in each panel denotes the $1/\sigma$-weighted mean value of $\log_{10}\rho\left(h_0\right)$ for each data set.

6. Comparison With Satellite Density Observations

Atmospheric density profiles for each MLS observation were obtained using the ideal gas law $\rho = p\left(R_s T\right)^{-1}$, where $R_s = 287.058$ J kg^{-1} K^{-1} is the specific gas constant of dry air. The density at h_0 for each coincident 6 h meteor observation block was determined by performing a quadratic interpolation to $\log\rho$ as a function of z in the vicinity of h_0. The larger time bin for radar/satellite comparisons was used to ensure sufficient meteor detections during the evening satellite observations, which are near the time of the minimum rate of meteor radar detections.

MLS values of atmospheric density at the height of meteor radar decay time gradient reversal are shown in Figure 3, which shows that h_0 occurs near the height at which $\rho = 1.26 \times 10^{-5}$ kg m^{-3}. The $1/\sigma$-weighted mean of the MLS values of $\log_{10}\rho\left(h_0\right)$ is -4.91 ± 0.06 for the ascending orbital leg and -4.90 ± 0.06 for the descending orbital leg. The comparison of h_0 with MLS densities over a representative year constructed from the decade 2005–2014 indicates that intraannual variation of the density at h_0 is negligible.

The correlation between the MLS constant density height and the meteor radar gradient reversal height can also be seen at smaller time scales. Figure 4 shows a comparison of 4 h average values of the meteor radar diffusion coefficient gradient reversal height and the height of the 1.26×10^{-5} kg m^{-3} density level estimated from MLS data. It can be seen that the meteor radar gradient reversal height closely follows the MLS density level height and that individual estimates of the gradient reversal height are consistent from bin to bin.

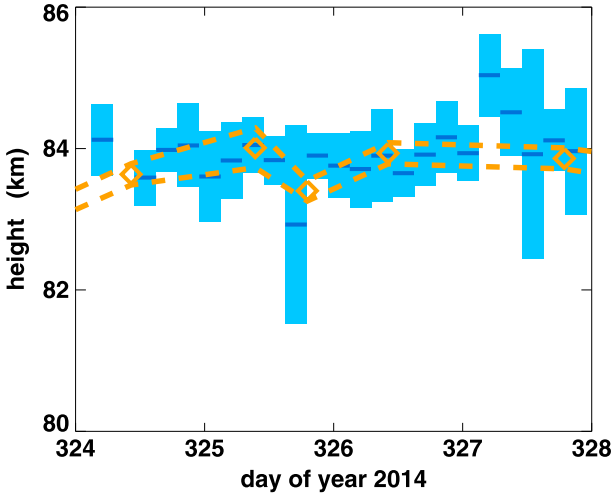

Figure 4. Comparison of 4 h averaged meteor radar diffusion coefficient gradient reversal heights (blue line segments; bars show one standard deviation) with the height of the 1.26×10^{-5} kg m^{-3} density level obtained from Aura MLS (orange diamonds; dashed lines show one standard deviation).

An advantage of using meteor radar to estimate the height of a constant density surface is illustrated in Figure 4. MLS obtains two measurements per day, at most, with some observing periods not resulting in reliable data. The meteor radar method, while having lower precision than MLS, is capable of providing data at significantly higher temporal resolutions.

7. Conclusions

A comparison of the gradient reversal height of meteor radar echo decay times with satellite measurements of atmospheric density shows that h_0 is an excellent proxy for the height of the 1.26×10^{-5} kg m^{-3} density level in the

MLT. This indicates that meteor radar can be used as a tool for measuring variations in the height of a constant density surface in the middle atmosphere. The high detection rates of modern meteor radars [see, e.g., *Lee et al.*, 2013] that can routinely exceed 30,000 meteors per day enable h_0 to be determined at time scales of a few hours.

Constant density surface height estimates provide an opportunity to study the climate and dynamics of the atmosphere in the MLT region, as well as having implications for the interpretation of airglow observations. Improvements to density profiles in the mesosphere/lower thermosphere will also assist in better understanding the dynamics of objects entering the atmosphere, including natural meteors and spacecraft.

Acknowledgments

This study has been supported by Australian Research Council grants DP0878144 and DP1096901 and ASAC grant 2325. The authors would like to thank the Aura MLS team for providing the geopotential height and temperature measurements used in this study. The authors would also like to thank Andrew Klekociuk and John French of the Australian Antarctic Division for their helpful discussions. Aura MLS data are available from http://disc.sci.gsfc.nasa.gov/Aura/data-holdings/MLS. Meteor radar data are available from the University of Adelaide and the Australian Antarctic Division upon request.

The Editor thanks Chris Meek and Chris Hall for their assistance in evaluating this paper.

References

Campbell-Brown, M. D. (2008), High resolution radiant distribution and orbits of sporadic radar meteoroids, *Icarus*, *196*, 144–163, doi:10.1016/j.icarus.2008.02.022.

Chilson, P. B., P. Czechowsky, and G. Schmidt (1996), A comparison of ambipolar diffusion coefficients in meteor trains using VHF radar and UV lidar, *Geophys. Res. Lett.*, *23*, 2745–2748, doi:10.1029/96GL02577.

Decker, B. L. (1986), World geodetic system 1984. Defense Mapping Agency Aerospace Center St Louis Afs Mo.

Herlofson, N. (1947), The theory of meteor ionization, *Rep. Prog. Phys.*, *11*, 444–454.

Hocking, W. K. (1999), Temperatures using radar-meteor decay times, *26*(21), 3297–3300.

Holdsworth, D. A. (2005), Angle of arrival estimation for all-sky interferometric meteor radar systems, *Radio Sci.*, *40*, RS6010, doi:10.1029/2005RS003245.

Holdsworth, D. A., D. J. Murphy, I. M. Reid, and R. J. Morris (2008), Antarctic meteor observations using the Davis MST and meteor radars, *Adv. Space Res.*, *42*, 143–154, doi:10.1016/j.asr.2007.02.037.

Jones, J., A. R. Webster, and W. K. Hocking (1998), An improved interferometer design for use with meteor radars, *Radio Sci.*, *33*(1), 55–66, doi:10.1029/97RS03050.

Kim, J.-H., Y. H. Kim, C. S. Lee, and G. Jee (2010), Seasonal variation of meteor decay times observed at King Sejong Station (62.22°S, 58.78°W), Antarctica, *J. Atmos. Sol. Terr. Phys.*, *72*(11–12), 883–889, doi:10.1016/j.jastp.2010.05.003.

Lee, C., Y. H. Kim, J.-H. Kim, G. Jee, Y.-I. Won, and D. L. Wu (2013), Seasonal variation of wave activities near the mesopause region observed at King Sejong Station (62.22°S, 58.78°W), Antarctica, *J. Atmos. Sol. Terr. Phys.*, *105–106*, 30–38, doi:10.1016/j.jastp.2013.07.006.

Lübken, F. J., A. Müllemann, and M. J. Jarvis (2004), Temperatures and horizontal winds in the Antarctic summer mesosphere, *J. Geophys. Res.*, *109*, D24112, doi:10.1029/2004JD005133.

McKinley, D. W. R. (1961), *Meteor Science and Engineering*, McGraw-Hill, New York.

Takahashi, H., T. Nakamura, K. Shiokawa, T. Tsuda, L. M. Lima, and D. Gobbi (2004), Atmospheric density and pressure inferred from the meteor diffusion coefficient and airglow O2b temperature in the MLT region, *Earth Planets Space*, *56*, 249–258, doi:10.1186/BF03353407.

Tsutsumi, M., T. Tsuda, T. Nakamura, and S. Fukao (1994), Temperature fluctuations near the mesopause inferred from meteor observations with the middle and upper atmosphere radar, *Radio Sci.*, *29*, 599–610.

Waters, J. W., et al. (2006), The Earth Observing System Microwave Limb Sounder (EOS MLS) on the Aura Satellite, *IEEE Trans. Geosci. Remote Sens.*, *44*(5), 1075–1092, doi:10.1109/TGRS.2006.873771.

Younger, J. P., C. S. Lee, I. M. Reid, R. A. Vincent, Y. H. Kim, and D. J. Murphy (2014), The effects of deionization processes on meteor radar diffusion coefficients below 90 km, *J. Geophys. Res. Atmos.*, *119*, 10,027–10,043, doi:10.1002/2014JD021787.